Enhanced Physical Properties of Cobalt Oxide Nanoparticles for Energy Storage Applications

Shoaib Akram [1,2]
https://orcid.org/0000-0002-7241-7724
Fazli Maula [1,3,4]
https://orcid.org/0009-0003-2002-4931
Fawad Ali [1,3,6]
https://orcid.org/0000-0003-1454-1433
Muneeb ur Rahman [1,3]
https://orcid.org/0000-0002-9995-6576
Osama Tariq Satti [1,3,5]
https://orcid.org/0009-0001-9405-9841
Imosobomeh L. Ikhioya [7]
https://orcid.org/0000-0002-5959-4427
ikhioyalucky@gmail.com

Abstract

Cobalt dioxide (CoO_2) nanostructured material was synthesised via a solid-state reaction using cobalt nitrate tetrahydrate ($Co(NO_3)_2 \cdot 4H_2O$) and sodium hydroxide (NaOH) as precursors. The resulting materials were fabricated into three distinct working electrodes and evaluated electrochemically in a three-electrode configuration using 3 M KOH as the electrolyte. Cyclic voltammetry revealed pronounced redox peaks, which confirmed Faradaic charge storage behaviour. At a scan rate of 10 $mV \cdot s^{-1}$, the specific capacitances of CoO_2 samples annealed at 25 °C, 250 °C and 300 °C were 223, 348 and 473 F g^{-1}, respectively. This indicated improved performance with increasing annealing temperature. X-ray diffraction patterns showed characteristic peaks corresponding to the (111), (112), (200), (211) and (311) planes, which confirmed the crystalline nature of the CoO_2 nanostructures. Annealing was found to significantly influence morphology, crystallinity and electronic properties, with the bandgap narrowing from 2.00 eV (unannealed) to 1.77–1.86 eV (annealed). These results demonstrate that thermal treatment enhances the electrochemical and structural properties of CoO_2, which highlights its potential as a high-performance electrode material for next-generation energy storage devices.

1 National Centre for Physics, Quaid-i-Azam University, Pakistan.
2 Department of Physics, University of Punjab, Pakistan.
3 National Institute of Vacuum Science and Technology, Pakistan.
4 Abdul Wali Khan University, Pakistan.
5 School of Manufacture Science and Engineering, Southwest University of Science and Technology, China.
6 College of Microscale and Optoelectronic, Shenzhen University China.
7 Department of Physics, Federal University Lokoja, Nigeria.

UNISA university of south africa PRESS
Nano-Horizons
Volume 4 | 2025 | #16471 | 12 pages
Nano-Horizons
https://doi.org/10.25159/3005-2602/16471
ISSN 3005-2602 (Online)

Keywords: Bandgap, cobalt, CV, optical, oxide, SEM, XRD.

Research Highlights

- The solid-state reaction was used to synthesise CoO_2 nanostructured material.
- For the unannealed material, the energy bandgap of CoO_2 is 2.00 eV, whereas for the annealed material it ranges from 1.77 to 1.86 eV.
- The estimated specific capacitances of CoO_2, CoO_2 (250 °C) and CoO_2 (300 °C) nanostructured material at scan rates of (10) mVs^{-1} is (223, 348 and 473) Fg^{-1}.

1 Introduction

Environmental pollution is a significant result of using non-renewable resources such as fossil fuels, which are becoming more expensive each year as reserves diminish [1], [2]. It is crucial to prioritise the development of sustainable green energy, such as wind and solar power [3]–[5]. Advancements in energy storage technology have enhanced the storage and transportation of electricity from renewable sources. Rechargeable batteries and supercapacitors have traditionally been the primary choices for storing chemical energy. Rechargeable lithium-ion batteries, widely used today, provide high voltage, energy density, and excellent safety [6]–[8]. As the demand for lithium-ion batteries rises, the availability of lithium resources is decreasing rapidly. Owing to its abundance and low cost, sodium, an alkali metal, has been receiving increasing attention in recent years. Sodium-ion batteries continue to face challenges due to their inadequate cycle performance [9]–[11]. Super capacitors (SCs) provide faster charging and discharging, higher power density, a longer lifespan, and safer operation in contrast to rechargeable batteries. Unfortunately, SCs suffer from low energy density. Overcoming low energy density in SCs often involves developing high-performance electrode materials. Energy storage systems have become indispensable in today's world because of the proliferation of mobile electronic devices, electric vehicles and new energy vehicles [12]–[15]. Electrochemical containers, known as SCs, are gaining attention for their safe operation, cycle performance, charging capacity and power density [16].

Transition metal materials, especially oxides, are widely preferred for electrode materials in SCs. Cobalt-based materials are advantageous for SCs because of their abundance, stable cycles, electroactive sites, high capacitance and strong conductivity. Cobalt(II,III) oxide (Co_3O_4) and other cobalt-based materials have undergone extensive research, resulting in notable progress. Cobalt oxide nanoparticles found in various nanostructures display special properties including semi-conductivity, piezoelectricity, and optical features [17], [18]. Cobalt oxide nanoparticles are being evaluated for various uses such as nano sensors, energy storage, cosmetics, nano-electronic and nano-optics.

Cobalt (II) and ammonium oxalate were prepared by Manteghi *et al*. [10] in their study to generate a cobalt oxalate complex. To manage the particle size, a surfactant such as CTAB and F-127 was utilised. To obtain nano cobalt oxide, the calcined precipitate was

characterised using FTIR, SEM, TEM and XRD techniques. The pure and nano-sized particles had an average size smaller than 40 nm. The Co_3O_4@Ni foam electrode (Co_3O_4@NF) attained a peak capacitance of 351 F g^{-1} in a 2 M KOH solution with a scan rate of 0.85 A g^{-1}. The electrode shows exceptional long-term stability; it retains almost 98.6% of its initial specific capacitance after 1 000 testing cycles.

Velhal *et al*. [16] successfully synthesised various Co_3O_4 nanostructures on Ni foam using a one-pot hydrothermal method combined with surface modification. The morphology of the Co_3O_4 varied depending on the surfactant used. This structure exhibited a high specific capacitance of 521.63 F g^{-1} and excellent cycling stability; it retained 95.29% of its initial capacitance after 3 000 charge–discharge cycles. The interconnected nanonetwork improved electronic conductivity and reduced ion diffusion resistance, which demonstrated the effectiveness of surface modification in enhancing supercapacitor performance.

The structure of cobalt oxide nanostructured materials comprises tiny cobalt oxide particles. Their applications are diverse and include batteries, supercapacitors and electro-catalysis. They are used in gas sensors, magnetic substances and materials used in photocatalysis.

CoO_2 contains cobalt in the +4-oxidation state, whereas CoO has Co^{2+} and Co_3O_4 contains both Co^{2+} and Co^{3+}. The higher oxidation state in CoO_2 leads to greater redox activity, which is critical for reversible lithium intercalation and deintercalation. CoO_2 typically forms a layered structure (α-$NaFeO_2$-type), which facilitates two-dimensional pathways for lithium-ion diffusion. This contrasts with the more complex spinel (Co_3O_4) or rock salt (CoO) structures, which are less favourable for fast Li^+ mobility. CoO_2 has a relatively high electronic conductivity due to its mixed-valent nature and metallic or semi-metallic behaviour, which enhance battery power capability [1], [3], [4]. CoO and Co_3O_4, by contrast, are more insulating and require conductive additives in electrode formulations. CoO_2-based materials (such as $LiCoO_2$ when lithiated) operate at higher voltages (~3.9–4.2 V vs. Li^+/Li), which deliver greater energy density. Its layered structure allows for efficient and reversible insertion/extraction of lithium ions, critical for rechargeable battery cycling. While fully delithiated CoO_2 can be unstable, partially delithiated phases retain good structural integrity, which makes them suitable for practical cycling when properly managed [5], [8], [9]. CoO_2's high oxidation state, layered structure, and electronic properties distinguish it from other cobalt oxides and make it particularly well suited to meet current challenges in energy storage, such as achieving higher energy density, better cycling performance and faster charging capabilities.

CoO_2 nanostructured material was synthesised via a solid-state reaction. This solid-state route was selected over other synthetic methods (sol-gel, hydrothermal, and chemical vapour deposition) [5], [8], [9]. The solid-state reaction requires no complex precursors, surfactants or solvents, which makes it a straightforward, low-cost method suitable for

producing CoO_2 at larger scales. The decomposition of $Co(NO_3)_2 \cdot 4H_2O$ in the presence of NaOH provides a localised high-temperature environment and reactive intermediates that facilitate the formation of Co^{4+} species, which promote the direct synthesis of CoO_2. This route enables the formation of nanostructured CoO_2 without the use of templating agents or solvents, which can introduce impurities or require complex post-synthesis treatments. Avoiding organic solvents and minimising waste aligns with greener synthesis practices, and enhances the sustainability of the method [1], [2], [5], [8], [9]. Overall, this approach leverages the thermally driven reactivity of the precursors to obtain nanostructured CoO_2 in a scalable, efficient manner. Its simplicity and effectiveness make it well suited for exploring CoO_2's potential in high-performance energy storage applications.

In this study, cobalt oxide nanostructured materials were synthesised with the aim of enhancing the physical properties of cobalt oxide nanoparticles for energy storage applications. The synthesised materials will be characterised using various techniques, including CV, optical analysis, structural characterisation, surface morphology imaging, and elemental composition analysis.

2 Experimental Procedure for CoO_2 Nanostructured Material

2.1. Chemicals Used in the Synthesis

The chemicals used for the synthesis of CoO_2 nanostructured material are: 1.5 g of cobalt nitrate tetrahydrate $Co(NO_3)_2 \cdot 4H_2O$ and 1.2 g of sodium oxide (NaOH). All chemicals obtained from Sigma Aldrich have a 99% purity level.

2.2 Synthesis of CoO_2 Nanostructured Material

The solid-state reaction was used to synthesise CoO_2 nanostructured material. Cobalt nitrate tetrahydrate $Co(NO_3)_2 \cdot 4H_2O$ and 1.2 g of sodium oxide (NaOH) were combined to produce CoO_2 nanostructured material. The chemicals were mixed with the salts and ground for 15 minutes, repeating the process twice. The initial calcination took 17 hours at a temperature of 950 °C, with a steady temperature increase of 10 °C per minute. To complete the second calcination, grind for 25 minutes twice and then heat at 10 °C/min for 17 hours at 950 °C. The powder was milled for two cycles of 25 minutes each before being heated to 1 200 °C for 12 hours, increasing the temperature by 10 °C per minute. Two separate annealing processes were conducted on the CoO_2 nanostructured material at 250 and 300 °C for 12 hours each (Fig. 1).

The Gamry Potentiostat and Galvanostat use specific electrodes, including a CoO_2 nanostructured material working electrode, a platinum counter electrode and an Ag/AgCl reference electrode. The Gamry Reference 3000, a Potentiostat/Galvanostat/ZRA with 32 V/1.5, was used for all electrochemical measurements at room temperature. The electrolyte consisted of a 3 M NaCl concentration. This procedure is followed to adequately prepare the working electrode. Mix CoO_2 nanostructured material, carbon black, and PVDF binder in NMP solvent to

create a slurry with a 90:5:5 ratio. The slurry was applied to nickel foam and allowed to dry overnight in an oven to enhance the bond between the active material and the current collector. The newly created electrode was employed for optical analysis and electrochemical measurements, such as cyclic voltammetry (CV). The crystal structures and orientations of both annealed and unannealed nanoparticles were examined using an X-ray diffractometer. We conducted our investigation in the 2theta range from 15 to 60°. SEM was used to analyse the morphology and elemental compositions. The optical properties of these materials were examined using a UV-visible spectrophotometer within the range of 300 to 1 000 nm.

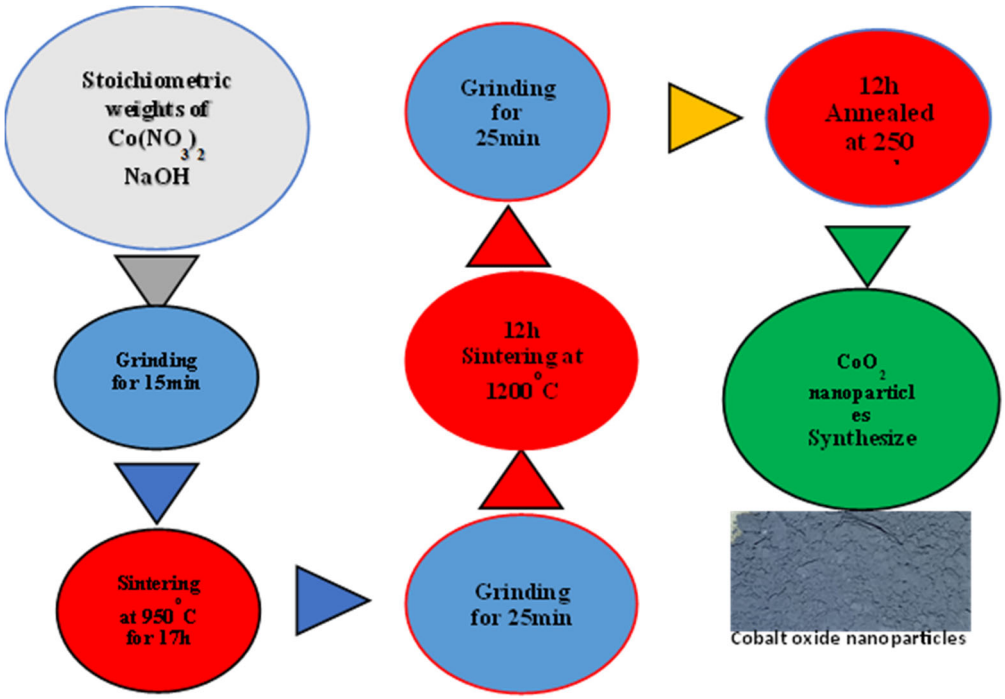

Fig. 1. Synthesis stages of CoO_2 nanostructured material.

3 Results

3.1 Cyclic Voltammetry Measurement of CoO_2, CoO_2 (250 °C), CoO_2 (300 °C) Nanostructured Material

Cyclic voltammetry was used to assess the electrochemical characteristics of CoO_2 nanostructured material, and to evaluate its super-capacitance properties (Fig. 2). A three-electrode system, which consisted of an Ag/AgCl reference electrode, a platinum counter electrode, and a working electrode on nickel foam, was employed for the electrochemical investigations. The three synthesised working electrodes were each tested individually using 3 M KOH as the electrolyte. By analysing the scan rate, the

electrodes' capacitance performance was evaluated using CV. Notable peaks at potential window of (−0.5 to 0.5) and a strong pseudo-capacitive potential were observed in the three electrodes, which were scanned at a range of 10 mVs^{-1}. By analysing a CV plot and utilising equation 1 [19], [20], it becomes feasible to differentiate between various capacitances.

$$C_{sP} = \frac{1}{2mk\Delta V} \int IdV \tag{1}$$

where C_{sP} is the specific capacitances, m is the active mass loaded on the electrode, k is the scan rate in mVs^{-1}, ΔV is the potential window, and $\int IdV$ is the integral of area under the CV curve.

The CV analysis of a three-electrode system revealed redox peaks, which indicated the presence of Faradaic processes. The estimated specific capacitances of CoO_2, CoO_2 (250 °C), CoO_2 (300 °C) nanostructured material at scan rates of (10) mVs^{-1} are (223, 348 and 473) Fg^{-1}. The material's pseudo-capacitive properties become apparent when its potential is measured and charges can rapidly transfer in both directions during Faradaic reactions. CoO_2 nanostructured material annealed at 300 °C demonstrated the highest specific capacitance.

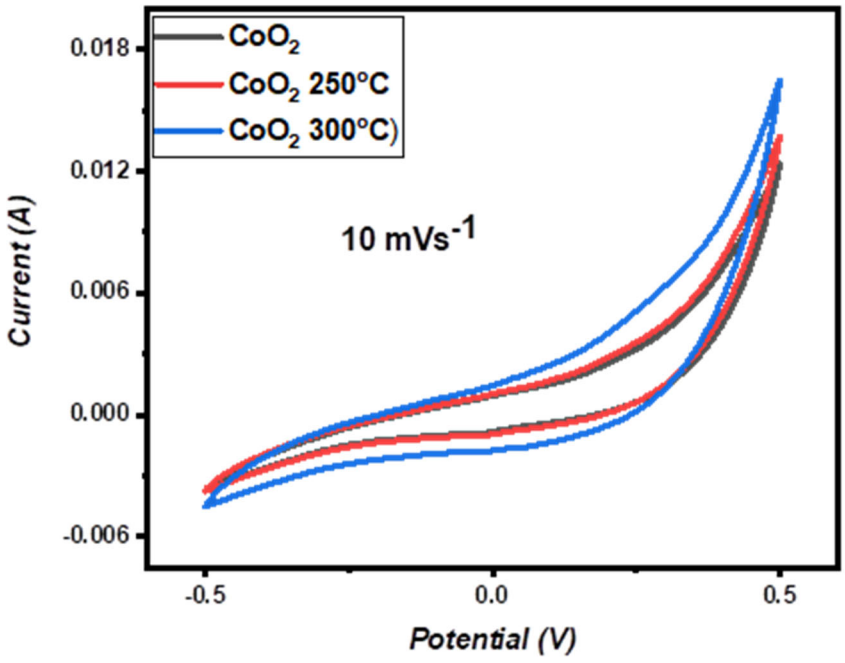

Fig. 2. Cyclic voltammetry of CoO_2, CoO_2 (250 °C), CoO_2 (300 °C) nanostructured material at scan rates of (10) mVs^{-1}.

3.2 XRD Analysis

The XRD study reveals the crystal structures of CoO_2 nanostructured material as presented in Fig. 3. The diffraction value of CoO_2 nanostructured material at $2\theta = 54.367°$ confirmed the characteristic peak of CoO_2 nanostructured material. The diffraction peaks at $2\theta = 26.264°$, 33.527°, 37.579°, 51.264° and 54.367° correspond respectively to the diffraction planes of 111, 112, 200, 211 and 311 of CoO_2 nanostructured material [21]–[23]. The crystallite size of the electrode material was calculated using equation 2 [24]–[32]:

$$D = \frac{k\lambda}{\beta cos\theta} \tag{2}$$

where k is 0.9 and λ is 0.12406 nm (wavelength of X-ray source) and β is the full width at half maximum in radians.

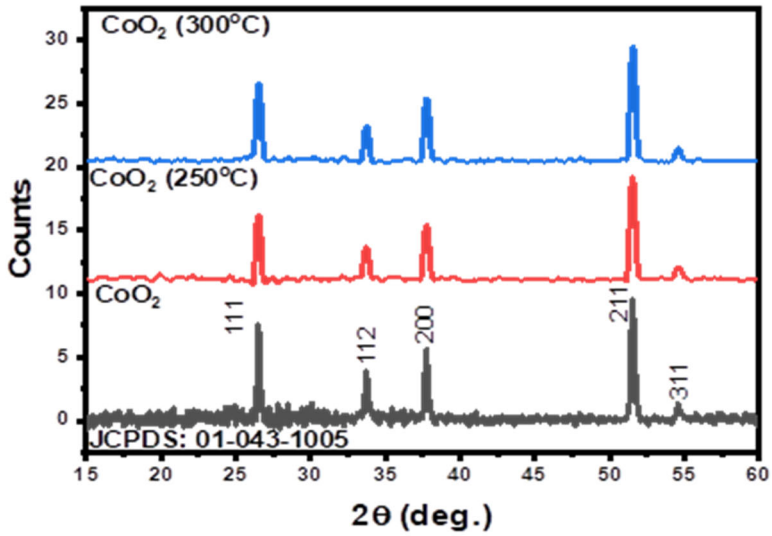

Fig. 3. XRD pattern of CoO_2 nanostructured material.

Table I presents the calculation of the crystallite size of CoO_2 nanostructured material. Altering the temperature between 250 and 300 °C causes structural changes in CoO_2 nanostructured material during annealing. This process influences the material's properties and performance. The CoO_2 nanostructured material's crystallite size grows as the annealing temperature rises. This suggests an improvement in the crystallinity and growth of the material's grains. By annealing CoO_2 nanostructured material at varying temperatures, the crystallite is improved. The presence of these crystallites has an impact on both the material and optical bandgap.

TABLE I
STRUCTURAL PROPERTIES OF CoO2 NANOSTRUCTURED MATERIAL

Material	2 theta (deg.)	D (spacing)	Å	β	hkl	D (nm)	**σ** (line/m^2) X 10^{15}
CoO_2	26.264	3.392	5.876	0.756	111	1.884	8.575
	33.527	2.672	5.344	0.758	112	1.911	8.333
	37.579	2.393	4.786	0.759	200	1.931	8.168
	51.264	1.781	3.984	0.762	211	2.019	7.466
	54.367	1.687	4.132	0.766	311	2.036	7.345
CoO_2 (250 °C)	26.768	3.329	5.767	0.843	111	1.692	1.064
	33.982	2.637	5.275	0.848	112	1.711	1.040
	38.043	2.364	4.729	0.849	200	1.728	1.019
	51.916	1.760	3.937	0.851	211	1.813	9.261
	54.782	1.675	4.103	0.853	311	1.832	9.074
CoO_2 (300 °C)	26.768	3.329	5.767	0.864	111	1.650	1.117
	33.982	2.637	5.275	0.866	112	1.675	1.085
	38.043	2.364	4.729	0.869	200	1.689	1.067
	51.916	1.760	3.937	0.872	211	1.769	9.724
	54.782	1.675	4.103	0.878	311	1.780	9.614

3.3 Surface Morphology

Fig. 4 reveals a distinctive surface morphology of the CoO_2 nanostructured material. The high surface area and porous structure of this material attribute to its enhanced electrochemical performance. The surface micrograph heavily influenced the behaviour of CoO_2 nanostructured material in various applications. The nano-ball within a micrograph of CoO_2 nanostructured material influences the capacitance and energy storage capacity of supercapacitors [22], [23]. Expanding the interlayer spacing of CoO_2 nanostructured material can enhance energy storage capabilities. The scalability of ultra-capacitors relies on the criticality of the surface of CoO_2 nanostructured material. The potential of CoO_2 nanostructured material for high-power and energy density is attributed to its high conductivity and specific surface area. CoO_2 nanostructured material is a superb option for supercapacitor electrodes. The CoO_2 nanostructured material exhibits a porous nano-ball surface structure, suggesting oxide in the Co electrode lattice [21]. Including oxide in the Co lattice structure enhances the surface micrograph of the Co electrode, resulting in improved energy storage capabilities. Fig. 5 displays the elemental analysis of CoO_2, including all the elements found in the materials.

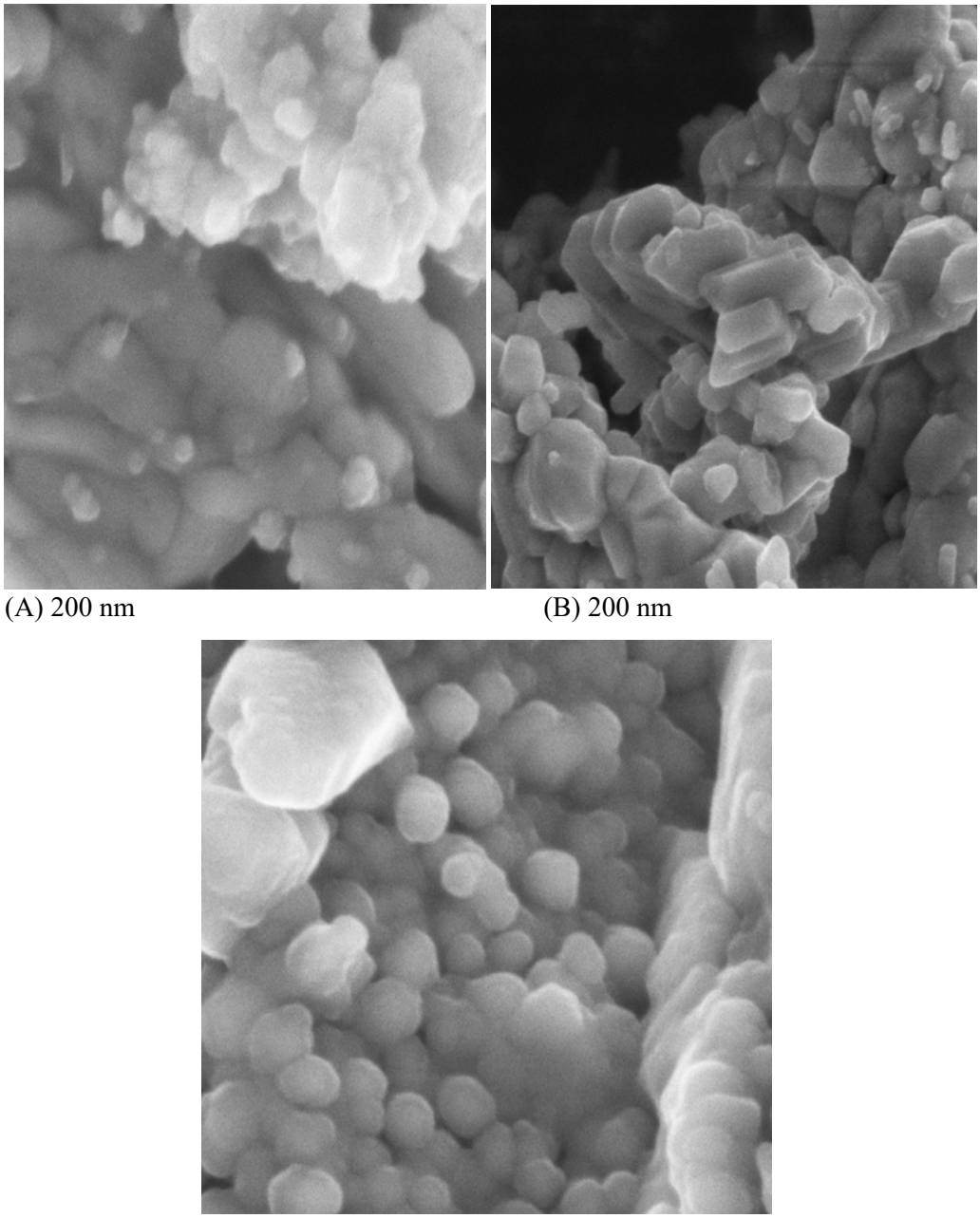

(A) 200 nm (B) 200 nm

(C) 200 nm

Fig. 4. SEM of CoO_2 nanostructured material (A) unannealed, (B) 250 °C, and (C) 300 °C.

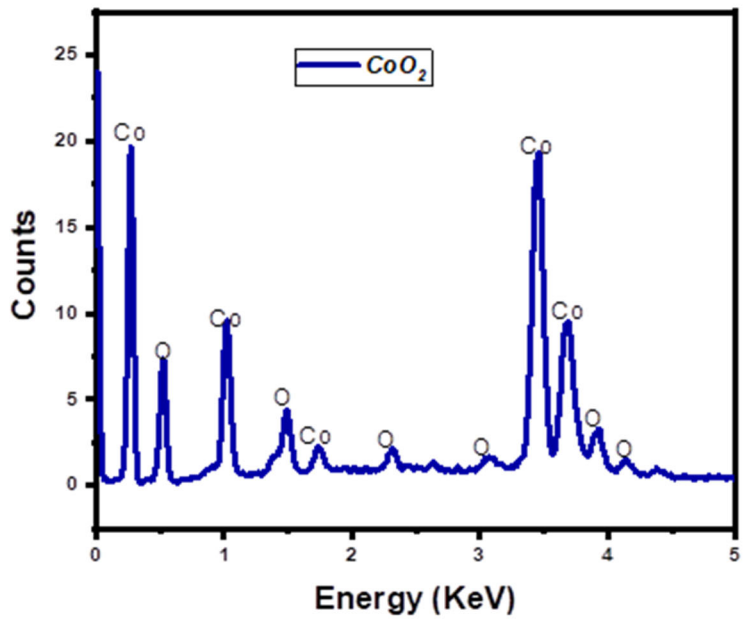

Fig. 5. EDXs of CoO_2 nanostructured material.

3.4 Optical Study

Fig. 6(a) shows the absorbance properties of CoO_2. The highest absorbance occurs in the CoO_2 material that has not been annealed, as it absorbs more energy in the visible region of the spectra. The absorbance of the annealed material decreases with increasing annealing temperature. CoO_2 nanostructured materials exhibit different absorbance properties depending on annealing temperatures of 250 and 300 °C. Alterations in the crystal structure, surface morphology and optical bandgap of the material cause the changes in absorbance. The annealing temperature significantly affects the absorbance of CoO_2 nanostructures. Increased annealing temperatures improve crystallinity, decrease defects and enhance optical properties. This leads to increased absorbance in the visible and near-infrared regions. Tailored absorbance properties make CoO_2 nanostructures useful in photocatalysis, energy storage and sensing. Their efficient light absorption makes them ideal for solar energy conversion, batteries and optoelectronic devices.

Fig. 6(b) shows the transmittance properties of CoO_2. The CoO_2 material that has not been annealed absorbs more energy in the visible region, which leads to the lowest transmittance. The transmittance of the annealed material increases as the annealing

temperature increases. The transmittance of CoO_2 nanostructured materials is affected by the annealing temperature. Increased transmittance is typically observed with higher annealing temperatures as a result of improved crystallinity and reduced defects. As the annealing temperature rises, the size of CoO_2 nanostructures also increases. Grain growth increases and grain boundaries decrease due to higher temperatures. By controlling the annealing temperature, one can adjust the optical properties of cobalt oxide nanostructures, including transmittance and absorption. This enables the creation of materials with tailor-made optical properties for different uses.

Fig. 6(c) illustrates the reflectance properties of CoO_2. Unannealed CoO_2 material has higher energy absorption in the visible region, which results in maximum reflectance. The reflectance of CoO_2 nanostructured material changes with annealing temperature (250 °C to 300 °C) due to alterations in its structural and optical properties. The reflectance of cobalt oxide nanostructured material is greatly affected by the annealing temperature. Increased annealing temperatures typically result in greater crystallinity and grain growth, which lead to improved reflectance. The CoO_2 nanostructured material undergoes structural and optical changes during the annealing process. The material's reflectance properties are affected by changes such as the formation of crystal phases and the modification of the bandgap.

Fig. 6(d) illustrates the bandgap energy of CoO_2. The investigation focused on the energy bandgap of CoO_2 nanostructured materials synthesised at various annealing temperatures ranging from 250 to 300 °C. The annealing temperature affects the energy bandgap of CoO_2 nanostructures. The bandgap energy decreases as the annealing temperature increases. The structural and morphological properties of CoO_2 nanostructures closely influence their energy bandgap. The annealing temperature, which affects the bandgap, can influence the size, shape and crystallinity of nanostructures. For the unannealed material, the energy bandgap of CoO_2 is 2.00 eV, whereas for the annealed material it ranges from 1.77 to 1.86 eV.

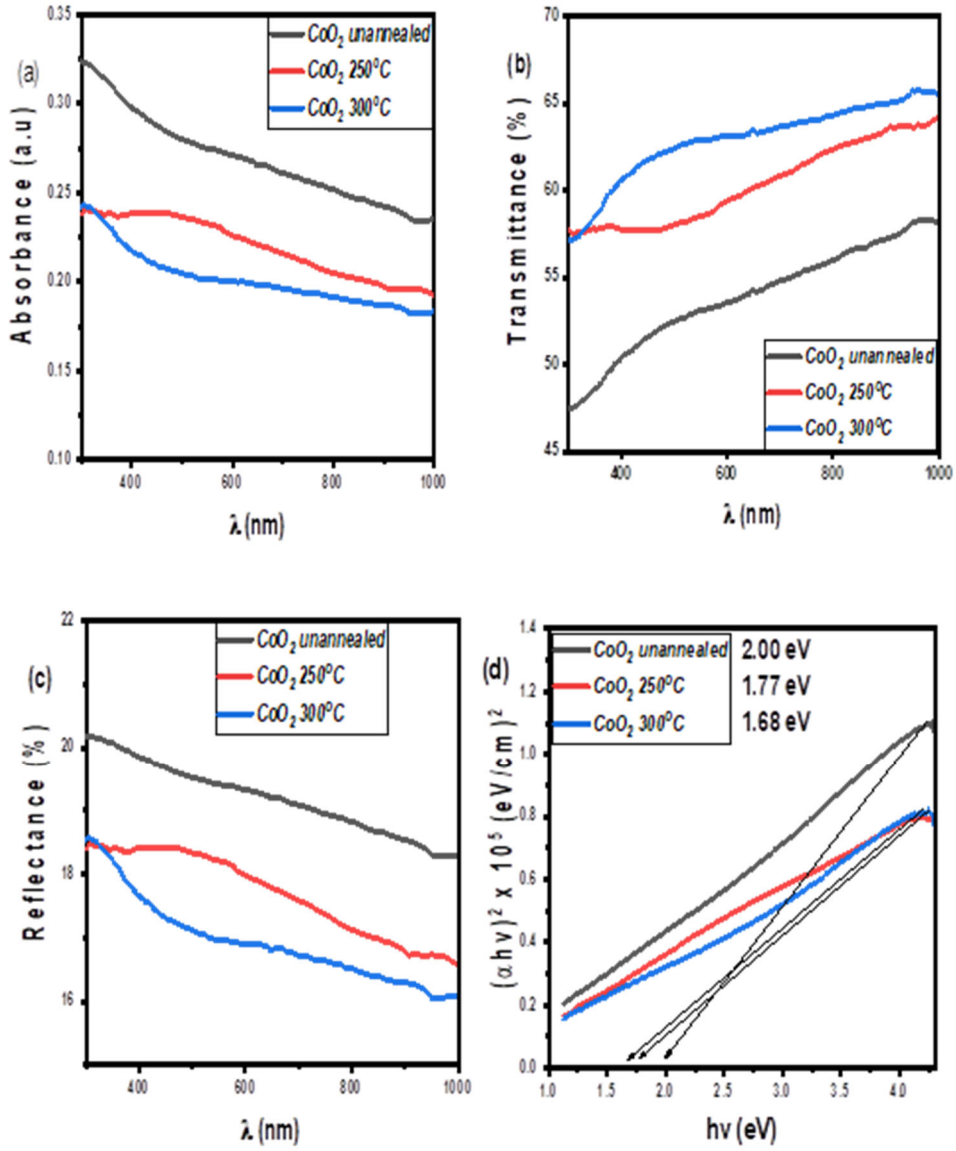

Fig. 6. UV-visible of CoO_2 nanostructured material (a) absorption spectra, (b) transmission spectra, (c) reflection spectra and (d) bandgap energy spectra.

3.5 Comparative Analysis of CoO_2 Nanostructured Materials for Energy Storage

In our study, CoO_2 nanostructured materials synthesised via a solid-state reaction demonstrated specific capacitances of 223 F g^{-1} (unannealed), 348 F g^{-1} (annealed at 250 °C), and 473 F g^{-1} (annealed at 300 °C) at a scan rate of 10 mV s^{-1}. These values

indicate a significant enhancement in electrochemical performance with increased annealing temperatures, which is attributed to improved crystallinity and conductivity. In contrast, Hettler *et al*. [33] synthesised CoO_2 nanoscrolls exhibiting exceptional electrical properties, including a high current-carrying capacity of 4×10^5 A cm^{-2} and a breakdown voltage of 270 kV cm^{-1}. While their study focused on electrical properties, it underscores the potential of nanostructured CoO_2 in high-performance applications. In comparison, Wang *et al*. [34] synthesised nanoporous Co_3O_4 nanorods via a hydrothermal method, which reported a specific capacitance of 280 F g^{-1}. Their study highlighted the significance of nanostructuring in enhancing electrochemical properties. Zhou *et al*. [35] improved the electrochemical performance of CoO nanoparticles by doping them with nickel, which increased the specific capacitance from 151.9 F g^{-1} to 279.5 F g^{-1} at a current density of 1 A g^{-1}. This improvement was ascribed to better mesoporosity and synergistic effects introduced by nickel doping.

CoO_2 nanostructures displayed diffraction peaks corresponding to planes (111), (112), (200), (211) and (311), which confirmed the formation of a well-defined crystalline structure. The annealing process not only enhanced crystallinity but also reduced the energy bandgap from 2.00 eV (unannealed) to a range of 1.77–1.86 eV, which facilitated better electronic conductivity. Similarly, the nanoscroll structures reported by Hettler *et al.* [33] achieved stability through curvature-induced strain, which maintained their structure over extended periods. This morphological stability is crucial to long-term energy storage applications. Similarly, Wang *et al*. [34] observed that their hydrothermally synthesised Co_3O_4 nanorods had a nanoporous structure consisting of aggregated nanocrystals, which contributed to enhanced electrochemical properties. Zhou *et al*. [35] nickel-doped CoO nanoparticles also demonstrated improved mesoporosity, which led to better electrochemical performance. The solid-state synthesis approach in our study, which utilised cobalt nitrate tetrahydrate and sodium hydroxide, offers a straightforward and scalable method for producing CoO_2 nanostructures. This contrasts with more complex methods such as the crystal conversion technique used by Hettler *et al*. [33], which, while effective, may present challenges in scalability. In contrast, Wang *et al*. [34] utilised a hydrothermal method to synthesise Co_3O_4 nanorods, which allowed for controlled morphology and porosity. Zhou *et al*. [35] adopted a solvothermal method for nickel doping in CoO nanoparticles, which enhanced their mesoporosity and electrochemical performance.

In our research, we contribute to the growing body of knowledge on CoO_2 nanostructured materials by demonstrating a scalable synthesis method that yields materials with enhanced electrochemical properties. The improvements in specific capacitance and conductivity, particularly with controlled annealing, position our CoO_2 nanostructures as promising candidates for energy storage applications. Our research contributes significantly to the development of CoO_2 nanostructured materials for energy storage applications. The solid-state synthesis method employed offers a scalable approach to producing materials with enhanced electrochemical properties. When compared to other studies, such as those by Hettler *et al*. [33], Wang *et al*. [34]

and Zhou *et al*. [35], our findings offer a balance between performance and practical synthesis considerations.

4 Conclusions

We have successfully used the solid-state reaction technique to synthesise CoO_2 nanostructured material. The three synthesised working electrodes were tested individually by using 3 M KOH as the electrolyte. The absorbance of the annealed material decreases with increasing annealing temperature. CoO_2 nanostructured materials exhibit different absorbance properties depending on annealing temperatures of 250 and 300 °C. Alterations in the crystal structure, surface morphology and optical bandgap of the material cause the changes in absorbance. The CV analysis of a three-electrode system revealed redox peaks, which showed Faradaic processes. The estimated specific capacitances of CoO_2, CoO_2 (250 °C), CoO_2 (300 °C) nanostructured material at scan rates of (10) mVs^{-1} is (223, 348 and 473) Fg^{-1}. The diffraction peaks at $2\theta = 26.264°$, 33.527°, 37.579°, 51.264° and 54.367° correspond respectively to the diffraction planes of 111, 112, 200, 211 and 311 of CoO_2 nanostructured material. The annealing temperature, which affects the bandgap, can influence the size, shape and crystallinity of nanostructures. For the unannealed material, the energy bandgap of CoO_2 is 2.00 eV, whereas for the annealed material it ranges from 1.77 to 1.86 eV.

5 References

[1] N. A. M. Barakat, M. S. Khil, F. A. Sheikh and H. Y. Kim, "Synthesis and Optical Properties of Two Cobalt Oxides (CoO and Co_3O_4) Nanofibers Produced by Electrospinning Process," *J. Phys. Chem. C*, vol. 112, no. 32, pp. 12225–12233, Jul. 2008, doi: 10.1021/jp8027353.

[2] A. S. Chang *et al*., "Highly Heterogeneous Morphology of Cobalt Oxide Nanostructures for the Development of Sensitive and Selective Ascorbic Acid Non-Enzymatic Sensor," *Biosensors*, vol. 13, no. 1, Jan. 2023, doi: 10.3390/bios13010147.

[3] J. S. Choi and C. H. Yo, "Study of the Nonstoichiometric Compositions of Cobaltous Oxide," *Inorg. Chem*., vol. 13, no. 7, pp. 1720–1724, Jul. 1974, doi: 10.1021/ic50137a037.

[4] M. Alheshibri *et al*., "Tailoring the surface morphology of nanostructured cobalt oxide for high-sensitivity CO sensor," *J. Mater. Sci*., vol. 57, no. 27, pp. 12865–12874, Jul. 2022, doi: 10.1007/s10853-022-07438-8.

[5] H. Eskalen, S. Kerli and Ş. Özgan, "Hydrothermally Produced Cobalt Oxide Nanostructures at Different Temperatures and Effect on Phase Transition Temperature and Threshold Voltage of Nematic Liquid Crystal Host," *Cobalt*, Dec. 2017, doi: 10.5772/intechopen.70946.

[6] P. S. Gaikar, A. P. Angre, G. Wadhawa, P. V. Ledade, S. H. Mahmood and T. L. Lambat, "Green synthesis of cobalt oxide thin films as an electrode material for electrochemical capacitor application," *Curr. Res. Green Sustain. Chem*., vol. 5, 2022, doi: 10.1016/j.crgsc.2022.100265.

[7] M. J. K. Reddy, S. H. Ryu and A. M. Shanmugharaj, "Synthesis of nanostructured lithium cobalt oxide using cherry blossom leaf templates and its electrochemical performances," *Electrochim. Acta*, vol. 189, pp. 237–244, Jan. 2016, doi: 10.1016/j.electacta.2015.12.079.

[8] S. Kuboon and Y. H. Hu, "Study of NiO-CoO and Co_3O_4-Ni_3O_4 Solid Solutions in Multiphase Ni-Co-O Systems," *Ind. Eng. Chem. Res*., vol. 50, no. 4, pp. 2015–2020, Jan. 2011, doi: 10.1021/ie101249r.

[9] J. Mei, T. Liao, G. A. Ayoko, J. Bell and Z. Sun, "Cobalt oxide-based nanoarchitectures for electrochemical energy applications," *Prog. Mater. Sci*., vol. 103, pp. 596–677, Jun. 2019, doi: 10.1016/j.pmatsci.2019.03.001.

[10] F. Manteghi, S. H. Kazemi, M. Peyvandipour and A. Asghari, "Preparation and application of cobalt oxide nanostructures as electrode materials for electrochemical supercapacitors," *RSC Adv*., vol. 5, no. 93, pp. 76458–76463, 2015, doi: 10.1039/c5ra09060a.

[11] R. K. Nare *et al*., "Sonication-supported synthesis of cobalt oxide assembled on an N-MWCNT composite for electrochemical supercapacitors via three-electrode configuration," *Sci. Rep*., vol. 12, no. 1, pp. 1–10, Feb. 2022, doi: 10.1038/s41598-022-05964-8.

[12] A. ul Rehman *et al*., "Enhanced Solar Cell Efficiency with Tin-Based Lead-Free Material (FASnl3) through SCAPS-1D Modeling," *Eurasian J. Sci. Technol*., vol. 4, no. 3, pp. 244–252, Jul. 2024, doi: 10.48309/ejst.2024.429200.1118.

[13] I. L. Ikhioya, N. Alghamdi, N. M. Ugwu, R. N. Odoh, S. E. Omeje, and D. C. Ikeh, "Fabrication of gadolinium oxide into the matrix of ZIF-67 via direct combination method for energy storage application," *Hybrid Adv.*, vol. 8, p. 100358, Mar. 2025, doi: 10.1016/j.hybadv.2024.100358.

[14] L. A. Nnannaa, U. Jospeh, E. C. Nwaokorongwu, U. A. Ezere, N. I. Akpu and I. L. Ikhioya, "Impact of annealing temperature on praseodymium cerium telluride nanoparticles synthesise via hydrothermal approach for optoelectronic application," *Mater. Res. Innov*., vol. 28, no. 6, pp. 448–459, Feb. 2024, doi: 10.1080/14328917.2024.2320982.

[15] N. Alghamdi and I. L. Ikhioya, "Improved efficiency of silver incorporation in the lattice of zirconium oxide via hydrothermal process for photovoltaic application," *J. Indian Chem. Soc.*, vol. 102, no. 6, p. 101719, Jun. 2025, doi: 10.1016/j.jics.2025.101719.

[16] N. B. Velhal, T. H. Yun, J. Ahn, T. Kim, J. Kim and C. Yim, “Tailoring cobalt oxide nanostructures for stable and high-performance energy storage applications,” *Ceram. Int*., vol. 49, no. 3, pp. 4889–4897, Feb. 2023, doi: 10.1016/j.ceramint.2022.10.003.

[17] C. Petrarca *et al*., “Cobalt magnetic nanoparticles as theranostics: Conceivable or forgettable?,” *Nanotechnol. Rev*., vol. 9, no. 1, pp. 1522–1538, Dec. 2020, doi: 10.1515/ntrev-2020-0111.

[18] R. S. Redekar *et al*., “Review on recent advancements in chemically synthesized manganese cobalt oxide ($MnCo_2O_4$) and its composites for energy storage application,” *Chem. Eng. J*., vol. 450, no. 1, Dec. 2022, doi: 10.1016/j.cej.2022.137425.

[19] A. Hussain, F. Ali and H. Hammad, “Enhanced specific capacitance , structural , optical , and morphological study of carbon ions incorporated into the lattice of $ZrCuO_2$ nanoparticle synthesized by hydrothermal method,” *Hybrid Adv*., vol. 5, p. 100170, Apr. 2024, doi: 10.1016/j.hybadv.2024.100170.

[20] I. L. Ikhioya and A. C. Nkele, “Green synthesis and characterization of aluminum oxide nanoparticle using neem leaf extract (*Azadirachta Indica*),” *Hybrid Adv*., vol. 5, p. 100141, Apr. 2024, doi: 10.1016/j.hybadv.2024.100141.

[21] A. J. Laghari *et al*., “Surface modification of Co_3O_4 nanostructures using wide range of natural compounds from rotten apple juice for the efficient oxygen evolution reaction,” *Int. J. Hydrogen Energy*, vol. 48, no. 41, pp. 15447–15459, May 2023, doi: 10.1016/j.ijhydene.2023.01.072.

[22] S. D. Karse and M. C. Fite, “Studies on structural and optical properties of cobalt oxide nanoparticles using co-precipitation,” *Phys. B Condens. Matter*, vol. 689, Sept. 2024, doi: 10.1016/j.physb.2024.416181.

[23] V. Adimule, S. DV, R. Joshi, A. K. Swetha, K. Sharma and R. Keri, “Influence of morphology, crystal structures on the enhanced photoluminescence dynamics, zeta potential, and AC resistance of disc shaped cesium oxide$_x$@cobalt oxide nanostructures,” *Results Opt*., vol. 17, Dec. 2024, doi: 10.1016/j.rio.2024.100742.

[24] S. G. Sarwar, I. L. Ikhioya, S. Afzal and I. Ahmad, “Supercapitance performance evaluation of MXene/Graphene/NiO composite electrode via in situ precipitation technique,” *Hybrid Adv*., vol. 4, p. 100105, Dec. 2023, doi: 10.1016/j.hybadv.2023.100105.

[25] H. Shah, S. Afzal, M. Usman, K. Shahzad and I. L. Ikhioya, “Impact of Annealing Temperature on Lanthanum Erbium Telluride (La0.1Er0.2Te0.2) Nanoparticles Synthesized via Hydrothermal Approach,” *Adv. J. Chem. Sect. A*, vol. 6, no. 4, pp. 342–351, Oct. 2023, doi: 10.22034/ajca.2023.407424.1386.

[26] K. I. Udofia, I. L. Ikhioya, D. N. Okoli and A. J. Ekpunobi, "Impact of doping on the physical properties of PbSe chalcogenide material for photovoltaic application," *Asian J. Nanosci. Mater*., vol. 6, no. 2, pp. 135–147, Jun. 2023, doi: 10.26655/AJNANOMAT.2023.2.3.

[27] I. L. Ikhioya *et al.*, "The effects of nitrogen ions' implantation on $La_{0.5}Ca_{0.5}MnO_3$ nanocomposite electrode for high-performance supercapacitor applications," *J. Mater. Sci.: Mater. Electron.*, vol. 36, no. 800, May 2025, doi: 10.1007/s10854-025-14859-z.

[28] I. Rufus, A. Peter, S. O. Aisida and I. L. Ikhioya, "Influence of manganese molarity incorporation on manganese silver sulphide semiconductor material for photovoltaic applications," *Results Opt*., vol. 12, p. 100464, Jul. 2023, doi: 10.1016/j.rio.2023.100464.

[29] S. O. Samuel, M. L. E. Frank, E. P. Ogherohwo, A. Ekpekpo, J. T. Zhimwang and I. L. Ikhioya, "Influence of Deposition Voltage on Strontium Sulphide Doped Silver for Optoelectronic Application," *East Eur. J. Phys*., vol. 1, pp. 189–196, Mar. 2023, doi: 10.26565/2312-4334-2023-1-25.

[30] I. O. Blessing, H. Shah, S. Afzal and I. L. Ikhioya, "Enhanced structural properties of electrochemically synthesised NiFeS using 500 keV carbon C^{++} ions irradiation," *Mater. Res. Innov*., vol. 28, no. 4, pp. 251–262, Jul. 2023, doi: 10.1080/14328917.2023.2262315.

[31] E. O. Ojegu, S. O. Samuel, M. O. Osiele, G. E. Akpojotor and I. L. Ikhioya, "Optimisation of deposition voltage of zirconium-doped chromium telluride via typical three-electrode cell electrochemical deposition technique," *Mater. Res. Innov*., vol. 28, no. 3, pp. 137–145, Aug. 2023, doi: 10.1080/14328917.2023.2243063.

[32] E. O. Ojegu, O. B. Odia, M. O. Osiele, A. E. Godfrey and I. L. Ikhioya, "Effect of precursor temperature on electrochemically deposited zirconium doped chromium telluride using a standard three-electrode system," *J. Mater. Environ. Sci.*, vol. 14, no. 11, pp. 1148–1159, 2023, https://www.jmaterenvironsci.com/Document/vol14/vol14_N11/JMES-2023-14113-Ojegu.pdf.

[33] S. Hettler, K. S. Roy, R. Arenal and L. S. Panchakarla, "Stable CoO_2 Nanoscrolls with Outstanding Electrical Properties," *Adv. Mater. Interfaces*, vo. 11, no. 31, Nov. 2024, doi: 10.1002/admi.202400317.

[34] G. Wang *et al*., "Hydrothermal Synthesis and Optical, Magnetic, and Supercapacitance Properties of Nanoporous Cobalt Oxide Nanorods," *J. Phys. Chem. C*, vol. 113, no. 11, pp. 4357–4361, Feb. 2009, doi: 10.1021/jp8106149.

[35] R. Zhou, X. Bi, X. Yuan, L. Zhang and Q. Huang, "Significant Improvement of the Electrochemical Performance of CoO Nanoparticles Through Activating Synergistic Effects by Doping with Nickel," *Eur. J. Inorg. Chem*., vol. 2020, no. 30, pp. 2889–2895, Aug. 2020, doi: 10.1002/ejic.202000357.